LAWRENCE
LIVERMORE
NATIONAL
LABORATORY

LLNL-JRNL-568532

Generation of Multi-charged High Current Ion Beams using the SMIS 37 Gas-dynamic Electron Cyclotron Resonance (ECR) Ion Source

M. Dorf, V. G. Zorin, A. V. Sidorov, A. F. Bokhanov, I. V. Izotov, S. V. Razin, V. A. Skalyga

August 1, 2012

Nuclear Instruments and Methods in Physics Research Section A

Disclaimer

Generation of Multi-charged High Current Ion Beams using the SMIS 37 Gas-dynamic Electron Cyclotron Resonance (ECR) Ion Source

M. A. Dorf[1], V. G. Zorin[2], A. V. Sidorov[2], A. F. Bokhanov[2], I. V. Izotov[2], S. V. Razin[2], and V. A. Skalyga[2]

[1]*Lawrence Livermore National Laboratory, Livermore, California, 94550 USA*

[2] *Institute of Applied Physics RAS, 46 Ulyanov St., 603950 Nizhny Novgorod, Russia*

A gas-dynamic ECR ion source (GaDIS) is distinguished by its ability to produce high current and high brightness beams of moderately charged ions. Contrary to a classical ECR ion source where the plasma confinement is determined by the slow electron scattering into an empty loss-cone, the higher density and lower electron temperature in a GaDIS plasma lead to an isotropic electron distribution with the confinement time determined by the prompt gas-dynamic flow losses. As a result, much higher ion fluxes are available, however a decrease in the confinement time of the GaDIS plasma lowers the ion charge state. The gas-dynamic ECR ion source concept has been successfully realized in the SMIS 37 experimental facility operated at the Institute of Applied Physics, Russia. The use of high-power (~100 kW) microwave (37.5 GHz) radiation provides a dense plasma (~10^{13} cm^3) with a relatively low electron temperature (~50-100 eV) and allows for the generation of high current (~1 A/cm^2) beams of multi-charged ions. In this work we report on the present status of the SMIS 37 ion source and discuss the advanced numerical modeling of ion beam extraction using the particle-in-cell code WARP.

I. INTRODUCTION

Progress in the development of ion sources toward increased beam current production while maintaining a tolerable beam emittance is of particular importance for heavy ion fusion (HIF) applications, where a high-current and high-brightness ion beam injector is required [1]. For the case of a plasma ion source, where an ion beam is extracted from a preformed plasma, an increase in the beam current is associated with an increase in the plasma density. In order to achieve high plasma density (n_p~10^{13} cm^3), the *gas-dynamic* ECR ion source SMIS-37 [2-4], built and operated at the Institute of Applied Physics,

Russia, utilizes high-power (~100kW) microwave (37.5 GHz) gyrotron radiation to produce an ECR discharge in the magnetically trapped plasma [Fig. 1]. The SMIS-37 source allows for the generation of high current (~1 A/cm^2) beams of moderately-charged heavy ions (e.g., N^{2+}) with a moderate transverse temperature (T_i~20 eV), and can have promising applications for the development of a HIF injector.

It is important to note that the regime of the plasma confinement in the SMIS-37 ion source is different from that in a *classical* ECR ion source [1]. In a low-density (n_p~10^{11}-10^{12} cm^{-3}) and high electron temperature (T_e~1 keV) plasma of a classical ECR ion source, the characteristic time of the Coulomb electron scattering into a loss-cone, $\tau_c=\ln R/\nu_{ei}$ is large compared to the gas-dynamic confinement time, $\tau_g=LR/V_s$. As a result, the electron loss cone is essentially empty, and the electron confinement time, τ_p is given by $\tau_c \approx \tau_p$ [5]. Here, R and L are the trap mirror ration and length, respectively, ν_{ei} is the electron-ion collision frequency, $V_s=(Z_i T_e/m_i)^{1/2}$ is the ion sound speed, T_e is the electron temperature, and m_i and Z_i are the ion mass and charge-state. Due to quasi-neutrality, the ambipolar electric field suppresses the ion losses from the trap (to the electron level), therefore limiting the extracted ion beam current. On the other hand, the efficient plasma confinement allows for the production of highly-charged ions due the electron impact ionization.

Contrary to the classical ECR source, for the parameters of the gas-dynamic source SMIS-37, characterized by a higher-plasma density (n_p~10^{13} cm^{-3}) and lower electron temperature T_e=50-100 eV, the gas-dynamic confinement time is large compared to the electron scattering time, i.e., $\tau_g >> \tau_c$. As a result, the electron distribution function is nearly isotropic, and the plasma losses are determined by the gas-dynamic plasma flows from the magnetic plugs, i.e., $\tau_c \approx \tau_g$. Therefore, the gas-dynamic regime of confinement allows for much higher ion fluxes from the magnetic plug (~1 A/cm^2), thus significantly increasing the extracted ion beam current. On the other hand, degraded confinement decreases the ion charge state. However, it is important to note that while using multi-charged ions can reduce the cost of the accelerating system, it will require a stronger-focusing transport system of the accelerator, and a higher plasma density in the neutralized drift section of a HIF driver. It is therefore likely that the optimal ion charge-

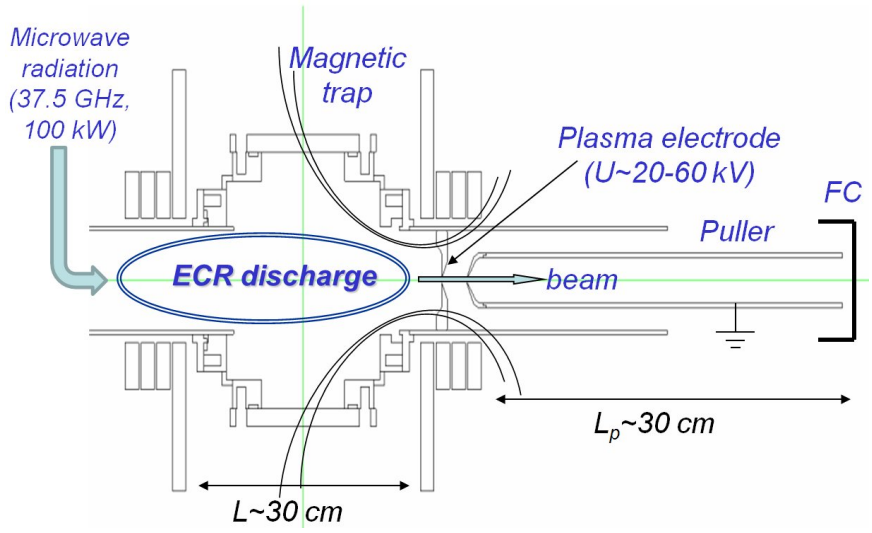

FIG 1. Schematic of the SMIS-37 gas-dynamics ECR ion source. The ECR plasma discharge is created by 37.5 GHz gyrotron radiation with a maximum power of 100 kW injected in pulses of 1.5 ms duration. The ECR plasma is confined in a magnetic trap with a maximum magnetic field B_m~2.5 T, and the gas-dynamic regime of plasma confinement is realized with the confinement time τ_g~10 μs. The two-electrode extracting system consists of a plasma electrode, part of the high-voltage plasma chamber housing, and a grounded extracting electrode (puller). The extracted current is measured by the Faraday cup situated immediately downstream of the puller's exit.

state should have a moderate value that can be achieved with a gas-dynamic ECR ion source.

Extensive experimental studies were carried out to characterize the performance of the SMIS-37 ion source using the nitrogen gas for the ECR plasma discharge [2-4, 6]. In particular, high ion fluxes from the magnetic plugs (~1 A/cm^2) with the ion-charge distribution peaked at N^{2+} were demonstrated [2], and the total beam current of ~150 mA was extracted by making use of the multi-aperture (13-hole) extraction system [6]. The pepper-pot method was used to measure the beam transverse emittance, demonstrating a single-beamlet emittance of ~10π mm×mrad [6]. Based on the emittance measurements an effective transverse ion temperature of ~20 eV was estimated [4], consistent with the theoretical predictions in Ref [7].

While very high ion fluxes are available from the magnetic trap of the SMIS-37 source, a large fraction can be lost at the surfaces of the extracting electrode. Therefore, the optimization of the ion beam extraction system is of particular practical importance. Accordingly, developing numerical capabilities for the modeling of ion beam extraction is needed. In the present work we report numerical simulations of the ion beam extraction

from the SMIS-37 ion source, performed using the particle-in-cell (PIC) code WARP [8] for the case of a single-aperture extraction system. The results of the numerical simulations are found to be in good agreement with the results of the experimental data, and provide insights into the SMIS-37 experiments.

II. SIMULATION MODEL

A schematic of the numerical simulations for the case of a single-aperture extraction is shown in Fig. 2. The self-consistent simulations are performed with the electrostatic version of the WARP code, neglecting the magnetic field effects on the ion beam extraction and assuming azimuthal symmetry for the Poisson equation. To model a plasma sheath layer we use a Boltzmann model for electrons, $n_e = n_{p0} \exp\left[e\left(\varphi - \varphi_p - U\right)/T_e\right]$, and set the three bounding conducting surfaces to the potential φ_p+U. Here, U is a high-voltage bias applied to the plasma chamber, φ_p is the plasma potential, φ is the electrostatic potential for which the Poisson equation is solved, n_{p0} is a constant corresponding to the plasma density at the left wall of the simulation domain, and e and T_e denote the electron charge and temperature, respectively. Though a direct measurement of the electron temperature is not available, a theoretical model has been developed that can estimate its value, T_e≈50-70 eV, from the measurements of the ion charge state distribution [3]. For all simulations presented in this work T_e=50 eV is assumed. The three ion species (N^+, N^{2+}, N^{3+}) are injected through the left wall of the simulation domain with the total charge density (summed over all species) equal to en_{p0}. The ratio of the species individual number densities, N^+ : N^{2+} : N^{3+} , used in the simulations corresponds to the results of the ion charge state distribution measurements. Consistent with the analysis in Ref. [7], we assume collisional ion flow and inject all species with the same directed velocity specified by the ion sound speed, $V_s = \sqrt{\left(\langle Z \rangle T_e + \gamma T_i\right)/m_i}$. Here, <Z> is the averaged ion charge, T_i is the ion temperature, and the adiabatic factor is taken to be γ=5/3. Following similar computational studies [1, 9], we approximate the plasma potential φ_p by requiring that the electron and ion current densities on the plasma chamber walls cancel each other. It is then straightforward to show that $\varphi_p = -0.5eT_e \ln\left[\left(2\pi m_e/m_i\right)\left(\langle Z \rangle + \gamma T_i/T_e\right)\right]$, where m_e is the

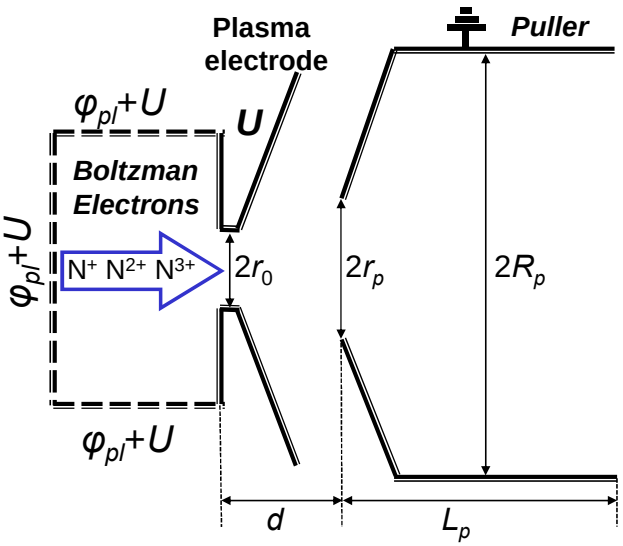

FIG 2. Schematic of the WARP simulations. The parameters of the simulations correspond to r_0=0.5 mm, r_p=1.5 mm, R_p=16 mm, L_p=26.1 cm, T_e=50 eV. The extraction voltage was varied in the range of 20-60 kV, and the distance between the plasma and extracting electrodes d was taken the values of 3 mm, 5 mm, and 7 mm. The extracted beam current (collected by the Faraday cup) was defined in the simulations as the ion current at the puller exit.

electron mass. Though this only approximates the plasma potential, our simulations demonstrated a weak dependence of the extracted current on its value. Note that the only free parameters of the simulation are the plasma density parameter, $n_{p0,}$ and the ion temperature, T_i, which we adjust to fit experimental data.

The beam ions are accelerated in the short gap (few millimeters) between the high-voltage plasma electrode and the grounded extracting electrode (hereafter referred to as puller). The beam then propagates through the long pipe (~25 cm) of the puller electrode and is collected by the Faraday cup at the puller exit (see Figs. 1-2). The entire simulation of the ion beam extraction is divided into two stages. For the first stage we perform a short-scale simulation of the ion beam extraction and acceleration: from the left plasma wall to just inside the puller. As a steady–state solution for the first-stage simulation is reached, the particle and field data are saved and used as the boundary condition for the second-stage (large-scale) simulation of the ion beam propagation through the puller pipe. Typical grid resolution for each of the simulations corresponds to 128 grid points in each (transverse and longitudinal) direction.

III. ION BEAM EXTRACTION: EXPERIMENTS AND SIMULATIONS

In this section we present the results of the numerical simulations demonstrating good agreement with the results of the measurements. However, let us first discuss qualitative features of the ion beam extraction from plasma [1]. The quality of the ion beam extraction strongly depends on the shape of the plasma boundary. The boundary (meniscus) can be either convex or concave (Fig. 3), depending on the ratio between the Bohm current, $j_B = en_{p0}V_s$ describing the ion flux from the quasi-neutral plasma, and the Child-Langmuir current, $j_{CL} = \sqrt{2\langle Z_i \rangle e/m_i}\, U^{3/2}/\left(9\pi d^2\right)$, limiting the value of the beam current in the vacuum acceleration gap. Here, *d* is the distance between the plasma and extracting electrodes. It is intuitively appealing to assume that the system (plasma - vacuum diode) will evolve in order to match the Bohm and Child-Langmuir currents. Accordingly, for the case of a dense plasma with $j_B > j_{CL}$, the plasma will "bulge out" (reducing the effective length of the vacuum gap "*d*", and therefore effectively raising the Child-Langmuir limit) leading to a convex plasma meniscus and a diverging ion beam (Fig. 3a). In the opposite case of a low-density plasma, $j_B < j_{CL}$, the plasma meniscus is concave leading to a converging ion beam. It is evident that both the premature focusing and strong divergence can lead to substantial beam losses on the surfaces of the extracting electrode (puller). Therefore, for each value of the plasma density there is an optimal value of the extracting voltage providing a maximum extracted beam current.

In the SMIS-37 facility, the extraction system can be moved within the expanding magnetic flux region (downstream of the magnetic plug) where the rapid decay of the plasma density occurs. Accordingly, the value of the ion current density leaving the plasma can be changed from ~1 A/cm^2 (corresponding to ~10 cm downstream of the plug) to ~100 mA/cm^2 (corresponding to ~20 cm downstream of the plug) [2]. We emphasize again, that due to imperfections in the extraction optics, a large fraction of that ion flux is typically lost on the puller before reaching the exit of the extraction system. Figures 4 (a) and 4(b) show the measurements of the extracted beam current, I_{FC} (collected by the Faraday cup), and the current collected by the puller, I_P, for the locations of the plasma electrode corresponding to 14 cm and 10 cm downstream of the magnetic plug, respectively. For these experiments a cusp-type configuration of the

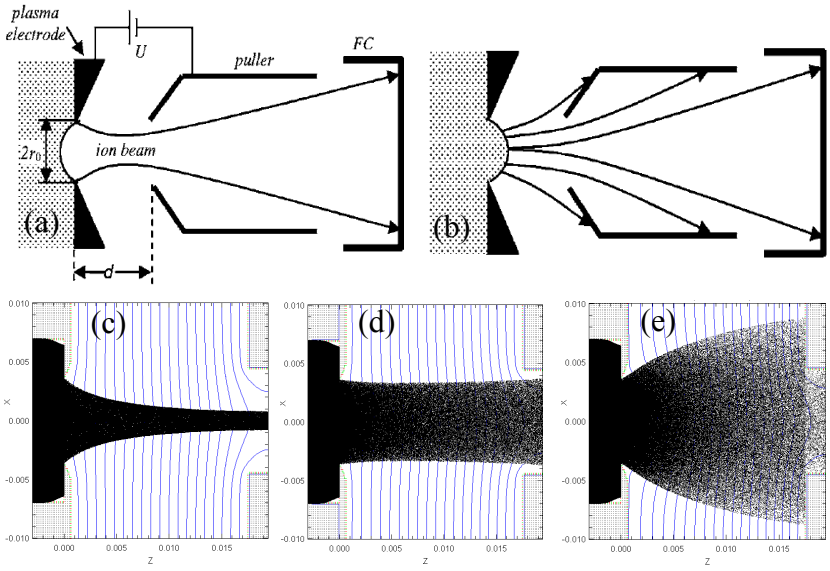

FIG 3. Qualitative features of the ion beam extraction from plasma. Frames (a) and (b) show schematic of the ion trajectories and the shape of the plasma meniscus for the cases of $j_B<j_{CL}$ and $j_B>j_{CL}$, respectively. Frames (c)-(d) show the results of the illustrative WARP simulations corresponding to (c) $j_B=0.53j_{CL}$, (d) $j_B=1.69j_{CL}$, and (e) $j_B=8.82j_{CL}$. Note that simplified beam-plasma parameters and extracting system geometry are used for the illustrative simulations in Frames (c)-(d), and do not correspond to that of the SMIS-37 ion source.

magnetic field was used, and the beam was extracted by making use of a one-aperture extraction system with r_0=0.5 mm, d=5 mm, r_p=3 mm (see Fig. 2). It is important to note that due to the secondary electron emission produced by the ion impact the current collected by the puller can be substantially larger than the ion current lost to the puller surface. The secondary electrons are accelerated by the positive ion charge toward the puller entrance and then are lost to the plasma or the plasma electrode. Therefore, the secondary electron emission contributes to the current drawn by the puller electrode, I_p. However, since the puller current is likely to be proportional to the ion flux absorbed by the puller surface, this measurement still characterize the efficiency of the extraction system.

The experimental results shown in Fig. 4 are in good agreement with the heuristic arguments mentioned earlier. Indeed, at low values of the extracting voltage, U, the Child-Langmuir current is much smaller than the Bohm current, therefore the extracted beam is diverging, and a significant fraction of the beam ions is lost to puller. As the extracting voltage increases the beam divergence is suppressed and the fraction of the ion beam transmitted to the Faraday cup increases as well. Furthermore, note that for the case

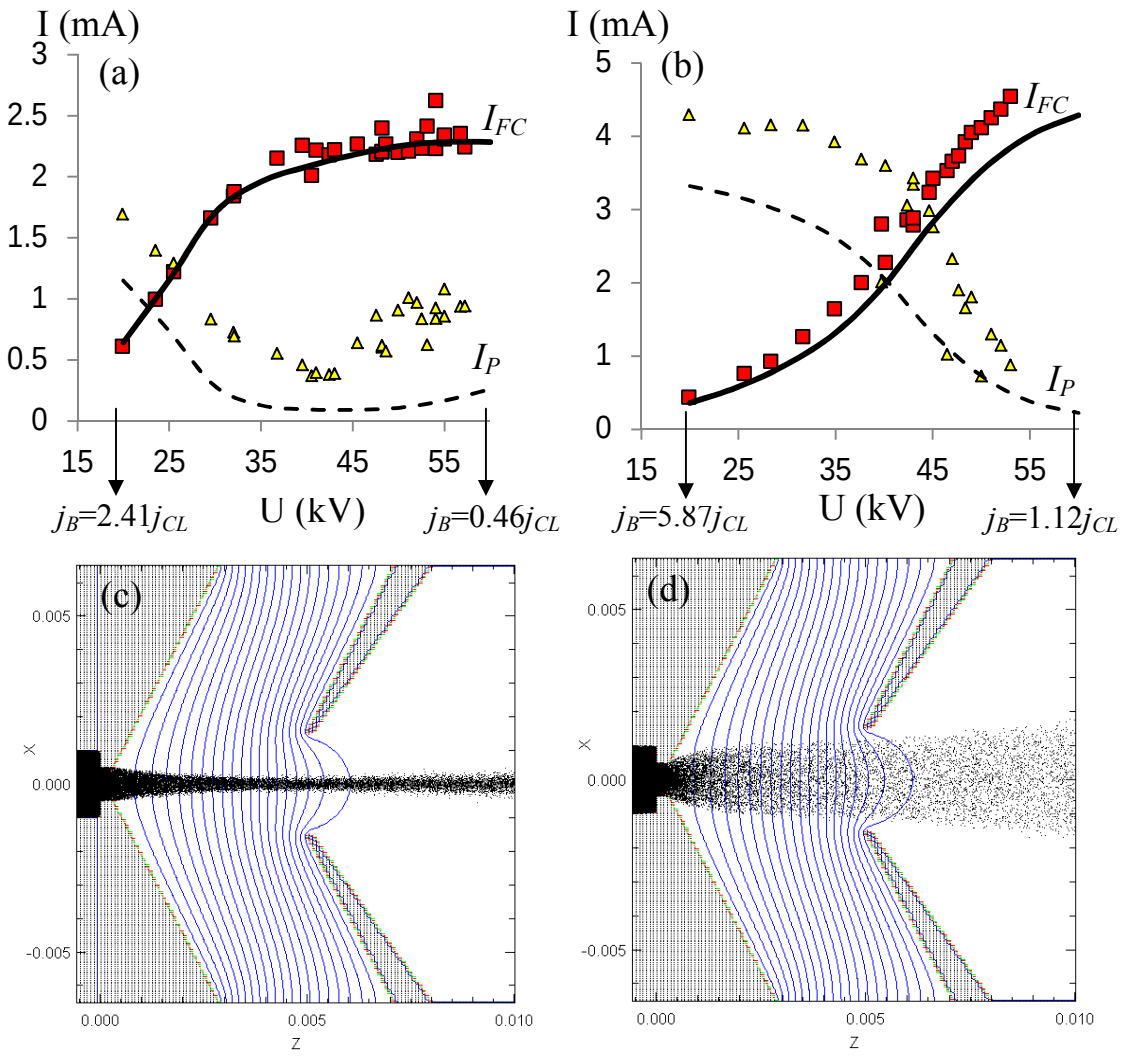

FIG 4. Beam extraction from the SMIS-37 ion source corresponding to d=3 mm. Frames (a) and (b) compare the results of the WARP simulations (solid and dashed curves) with the experimental data (squares and triangles) for the extracted (squares and solid curves) and puller (triangles and dashed curves) currents. Also shown is the relationship between the Bohm and Child-Langmuir currents for U=20 kV and U=60 kV. The distance between the plasma electrode and the magnetic plug corresponds to 14 cm (a) and 10 cm (b), and the species number densities are related as (a) N^+:N^{2+}:N^{3+}=0.48:0.43:0.09 , and (b) N^+:N^{2+}:N^{3+}=0.58:0.38:0.04 . The free parameters used in the WARP simulations correspond to (a) $n_{p0}=1.1\times10^{12}$ cm^{-3} and T_i=10 eV , and (b) $n_{p0}=2.7\times10^{12}$ cm^{-3} and T_i=10 eV. Frames (c) and (d) illustrate the ion trajectories obtained in the WARP simulations with [$n_{p0}=1.1\times10^{12}$ cm^{-3}, T_i=10 eV, U=60 kV] and [$n_{p0}=2.7\times10^{12}$ cm^{-3}, T_i=10 eV, U=20 kV], respectively.

of a lower plasma density [Fig. 4(a)] the optimal value of the extracting voltage corresponding to j_{CL}~j_B is reached, and the saturation of the extracted beam current, I_{FC} is observed. For the case of a higher plasma density [Fig. 4(b)], the high value of the ion

Bohm current leaving the plasma cannot be matched by the available extracting voltage (U<55 kV), and the current saturation does not occur.

The results of the numerical simulations (see Fig. 4) demonstrate good quantitative agreement with the experimental data. Comparing Figs. 4(a) and 4(b) we note a significant increase in the value of the plasma density parameter, n_{p0} (chosen to fit the experimental value), which is consistent with the plasma electrode being closer to the magnetic plug. As mentioned earlier, the measurements of the puller current include a substantial secondary electron current. The puller current obtained in the simulations includes only the ion flux absorbed by the puller surface, and therefore a close matching of the experimental data should not be expected. However, the $I_P(U)$ still describes the efficiency of the extraction system, and therefore has features similar to those of the experimental curve. Also note that the secondary electrons are rapidly lost from the extraction system, and therefore their influence on the ion beam dynamics can be neglected due to lack of space-charge accumulation. Accordingly, the secondary electrons have not been included in the WARP simulations.

It is interesting to investigate the influence of the ion temperature (a free parameter of the simulation) on the characteristics of the beam extraction. The results of the simulations shown in Fig. 5 demonstrate a strong ion temperature dependence for the puller current, I_P, and much weaker dependence for the extracted current, I_{FC}.

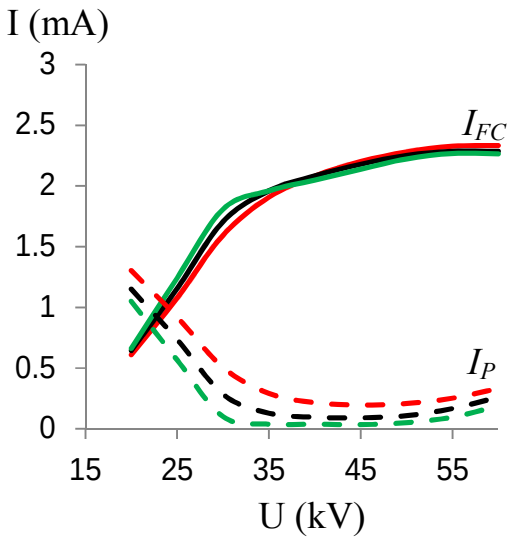

FIG 5. Influence of the transverse ion temperature on the characteristics of the beam extraction. Shown are the results of the WARP simulations for the extracted (solid curves) and puller (dashed curves) currents obtained for T_i=20 eV (red), T_i=10 eV (black), and T_i=4 eV (green). The system parameters are the same as in Fig. 4 (a).

Finally, we present the comparison between the simulations and the experimental data obtained for different values of the acceleration gap, d (Fig. 6). For these experiments the plasma electrode was positioned 10 cm downstream of the magnetic plug [same as in Fig. 4(b)]. Taking into account fluctuations in plasma parameters that may occur along with replacements of the extraction system, the agreement is very good.

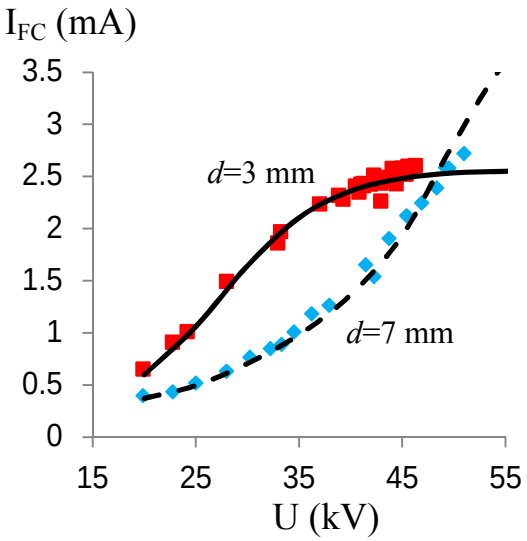

FIG 6. Influence of the acceleration gap, d, on the characteristics of ion beam extraction. Shown are the results of the WARP simulations (solid and dashed curves) and the experimental data (squares and diamonds) for the extracted beam current, I_{FC}, corresponding to d=3 mm and N^+:N^{2+}:N^{3+}=0.53:0.44:0.03 (red squares and solid curve) and d=7 mm and N^+:N^{2+}:N^{3+}=0.49:0.49:0.02 (blue diamonds and dashed curve). The ion temperature assumed in the WARP simulations is T_i=10 eV, and the plasma density parameter corresponds to $n_{p0}=2.4\times10^{12}$ cm^{-3} for d=3 mm and $n_{p0}=2.8\times10^{12}$ cm^{-3} for d=7 mm. The distance between the magnetic plug and the plasma electrode is 10 cm.

IV DISCUSSION

In the present work we reported on the modeling of the ion beam extraction system implemented in the SMIS-37 ion source. Numerical simulations including the self-consistent effects of the beam space-charge were performed using the WARP (PIC) code, and the results of the simulations were found to be in good agreement with the experimental data.

While the present studies described the generation of a high-current multi-charged nitrogen ion beam, it is important to note that the SMIS-37 ion source facility has also

been used for other applications. Recent experimental studies have investigated generation of a high-current hydrogen beam, which is of particular importance for a variety of applications including neutron production for boron neutron capture therapy. The use of high-power (~100 kW) microwave (37.5 GHz) gyrotron radiation allowed the creation of a high-density ECR plasma discharge in a hydrogen gas, and a high-current (~200 mA) proton beam was extracted [10]. Finally, we note that even higher-frequency (~1 THz) high-power (0.6 kW) radiation (produced by a large orbit gyrotron) has been recently employed at the SMIS-37 facility to create a small-volume argon plasma discharge with a linear dimension of a few millimeters and a density more than 10^{15} cm^{-3} [11]. This novel plasma discharge can have promising applications for the development of a high-intensity small-size source of multi-charged ions.

AKNOWLEDGEMETNS

The authors are grateful to Dave Grote for his expert services in implementation of the WARP code, and to Matthew Levy for careful reading of the manuscript. This research was supported by USDOE contract no. DE-AC52-07NA27344; Russian Foundation for Basic Research (RFBR), grant n0. 11-02-97056-r_povolzhie_a; Federal Targeted Program "Scientific and Educational Personnel of the Innovative Russia" for 2009-2013; President of the Russian Federation for young candidates of science grant n0. MK-4743.2012.2. LLNL-JRNL-568532

[1] *The Physics and Technology of Ion Sources*, edited by G. Brown (Wiley, New York, 2004).

[2] A. Sidorov A. Sidorov, A. Bokhanov, I. Izotov, S. Razin, V. Skalyga, and V. Zorin, A. Balabaev and S. Kondrashev, R. Geller, T. Lamy, P. Sortais, and T. Thuillier, P. Spädtke, Rev. Sci. Instrum. **77**, 03A341 (2006).

[3] V. Skalyga, V. Zorin, I. Izotov, S. Razin, A. Sidorov, and A. Bohanov, Plasma Sources Sci. Technol. **15**, 727 (2006).

[4] A. Sidorov, M. Dorf, V. Zorin, A. Bokhanov, I. Izotov, S. Razin, and V. Skalyga, J. Roßbach and P. Spädtke, A. Balabaev, Rev. Sci. Instrum. **79**, 02A317 (2008).

[5] V. Semenov, V. Skalyga, A. Smirnov, and V. Zorin, Rev. Sci. Instrum. **73**, 635 (2002).

[6] A. V. Sidorov, V. G. Zorin, I. V. Izotov, S. V. Razin, and V. A. Skalyga, Thecnical Physics **55**, 1540 (2010)

[7] M. Dorf, V. Semenov, and V. Zorin, Phys. Plasmas **15**, 093501 (2008).

[8] D. P. Grote, A. Friedman, I. Haber, W. Fawley, and J.-L. Vay, Nucl. Instrum. Methods Phys. Res. A **415**, 428 (1998).

[9] R. Becker and W. B. Herrmannsfeldt, Rev. Sci. Instrum. **63**, 2756 (1992).

[10] A. Sidorov *et al*., to be submitted (2012).

[11] V. L. Bratman, V. G. Zorin, Yu. K. Kalynov, V. A. Koldanov, A. G. Litvak, S. V. Razin, A. V. Sidorov, and V. A. Skalyga, Phys. Plasmas **18**, 083507 (2011).